CrossMark
click for updates

View Article Online
View Journal

RSC Advances

This article can be cited before page numbers have been issued, to do this please use: P. Sahatiya and S. Badhulika, *RSC Adv.*, 2015, DOI: 10.1039/C5RA15351D.

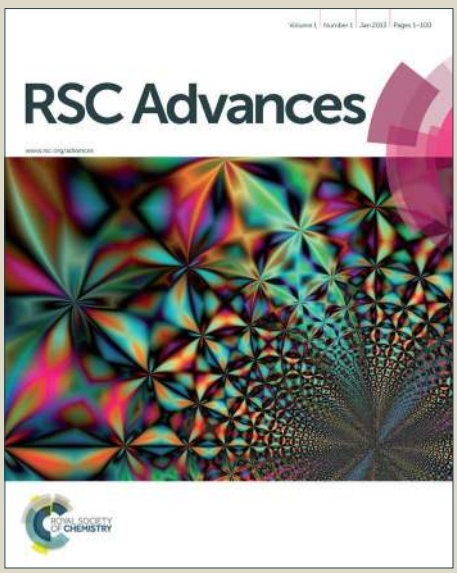

This is an *Accepted Manuscript*, which has been through the Royal Society of Chemistry peer review process and has been accepted for publication.

Accepted Manuscripts are published online shortly after acceptance, before technical editing, formatting and proof reading. Using this free service, authors can make their results available to the community, in citable form, before we publish the edited article. This *Accepted Manuscript* will be replaced by the edited, formatted and paginated article as soon as this is available.

You can find more information about *Accepted Manuscripts* in the Information for Authors.

Please note that technical editing may introduce minor changes to the text and/or graphics, which may alter content. The journal's standard Terms & Conditions and the Ethical guidelines still apply. In no event shall the Royal Society of Chemistry be held responsible for any errors or omissions in this *Accepted Manuscript* or any consequences arising from the use of any information it contains.

ROYAL SOCIETY OF CHEMISTRY

www.rsc.org/advances

View Article Online
DOI: 10.1039/C5RA15351D

Published on 16 September 2015. Downloaded by UNIVERSITY OF NEBRASKA on 16/09/2015 15:31:34.

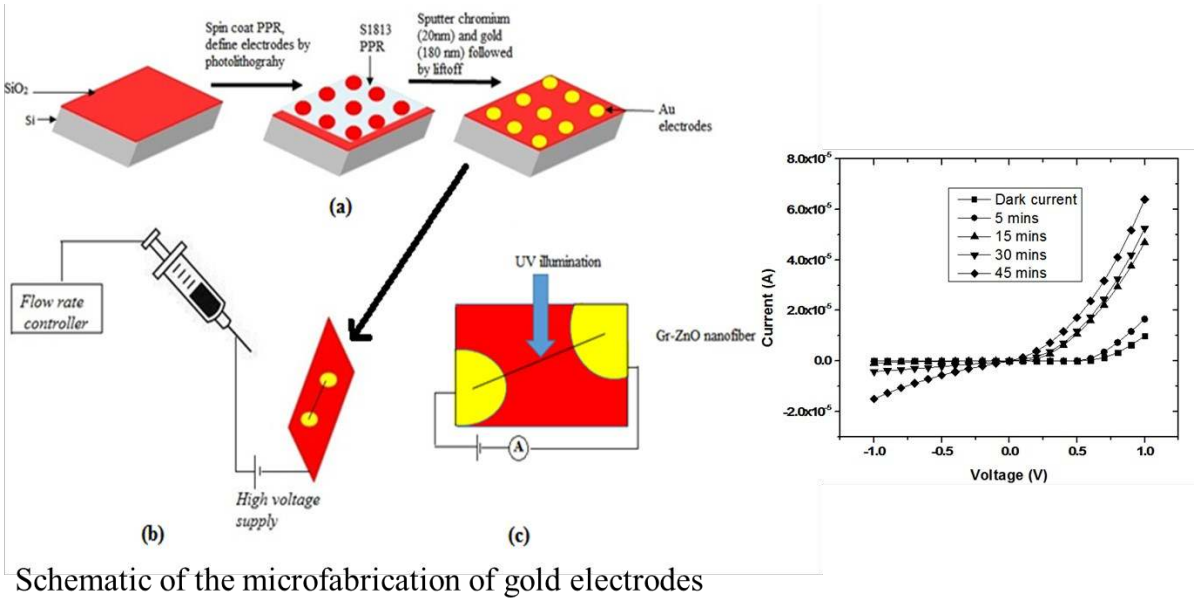

a) Schematic of the microfabrication of gold electrodes
b) Electrospinning with collector as pre patterned electrode
c) UV sensing with single aligned Gr-ZnO nanofiber device.

RSC Advances Accepted Manuscript

View Article Online
DOI: 10.1039/C5RA15351D

Journal Name

ARTICLE

Published on 16 September 2015. Downloaded by UNIVERSITY OF NEBRASKA on 16/09/2015 15:31:34.

Received 00th January 20xx,
Accepted 00th January 20xx

DOI: 10.1039/x0xx00000x

www.rsc.org/

One step in situ single aligned Graphene-ZnO nanofiber for UV sensing

Parikshit Sahatiya,[a] and Sushmee Badhulika[a]†

Herein we report a simple, one step method for in-situ synthesis and alignment of a single graphene doped Zinc oxide (Gr- ZnO) composite nanofiber fabricated by electrospinning across electrodes and its subsequent use for ultraviolet (UV) detection. The study involves the optimization of calcination temperature and time dependent electrospinning for alignment of Gr-ZnO composite nanofiber across gold electrodes. SEM analysis and Raman studies revealed the presence of ZnO embedded within uniformly distributed Gr flakes throughout the surface of the composite fiber. XRD of Gr-ZnO confirmed highly crystalline ZnO structure with amorphous graphene. Different weight percentages of graphene flakes were taken to synthesize the composite to determine the optimum composition that enabled the synergistic contribution of both ZnO and graphene for UV sensing. I-V measurements under UV illumination showed the composite to exhibit superior UV sensing performance with a ~1892 fold increase in the conductance for 0.5 wt. % of graphene. Underlying mechanism of charge transfer of photogenerated electrons and holes from ZnO to graphene under UV illumination was studied. The method presented in this paper provides a simple, effective and economic viable strategy for alignment of various composite fibers and can thus be used in a wide range of sensing applications.

1 Introduction

Near ultra violet detection is important for many applications such as environmental monitoring[1], military applications[2], flame detection[3] and industrial quality control[4]. In this regard, 1D Zinc oxide (ZnO) nanostructures find wide usage mainly due to its extraordinary electronic properties which include room temperature high bandgap of 3.37 eV[5], high exciton binding energy of 60mV[6], and high photoelectric properties by means of electron-hole generation or recombination during UV illumination. In addition, ZnO nanofiber based UV sensors have shown high on –off ratio and fast response[7]. To further enhance the properties and to expand its application pool, efforts have been made to synthesize ZnO hybrids. *Hoa et al*[8] synthesized 2D NiO sheets and 1D ZnO composite by hydrothermal process for enhancing sensitivity of UV sensor. *Li et al*[9] reported polymer/ZnO hybrid for wavelength selective response for near UV sensors. *Xi et al*[10] electrospun ZnO/SiO_2 nanofiber mat for flexible UV sensor. 1D ZnO hybrids exist in different morphologies such as nanorods[11], nanowires[12] and nanofibers[13] which can be synthesized using various methods such as chemical vapour deposition[14], hydrothermal[15], electrochemical deposition[16] and electrospinning[17]. Among the methods mentioned, electrospinning is simple and economic viable technique for

[a] *Indian Institute of Technology Hyderabad, Hyderabad 502205, India*
† Email: sbadh@iith.ac.in; *Telephone: 040-23018443 Fax 040-23016032*

RSC Advances Accepted Manuscript

Please do not adjust margins
View Article Online
DOI: 10.1039/C5RA15351D

Published on 16 September 2015. Downloaded by UNIVERSITY OF NEBRASKA on 16/09/2015 15:31:34.

synthesizing 1D ZnO hybrid nanofibers. More importantly, the electrospun nanofibers are continuous, easy to align from wide range of materials which could be processed into applications. The main challenge in fabrication of single nanofiber based device is their precise positioning between the electrodes and establishing an effective near ohmic or ohmic contact. In most cases, nanofibers are first synthesized and then metal contacts are carefully positioned at their ends by E-beam lithography[18]. However, such techniques are complex, result in low throughput and thus hinder the practical applicability of the senor.

In this study, we report one step in situ synthesis and alignment of single graphene doped ZnO nanofiber by the use of electrospinning. Graphene a two dimensional carbon monolayer has gained much attention in electronics and optoelectronics because of its excellent charge carrier transport mobility, high electrical conductivity, high optical transmittance and high mechanical stability[19]. Apart from these mentioned properties, its work function plays an important role in fabricating a UV sensor when used in conjunction with ZnO as graphene's work function being less than conduction band of ZnO allows the transfer of photogenerated electrons to graphene. We demonstrate time, which in this case is defined as the duration of operation of electrospinning, to be a vital parameter for alignment of a single nanofiber between the pre patterned electrodes. Our key strategy involves optimization of the operating time for fabricating a single aligned Gr-ZnO nanofiber device in a controllable and reproducible manner. By varying the operating time, the number of fibers deposited between the electrodes could be controlled. The device was then evaluated for UV detection. Unlike conventional ZnO based UV sensors which suffer from recombination of charge carrier related issues, this approach utilizes the excellent transport properties and high optical transmittance of graphene to enhance the performance of the UV sensor. To the best of our knowledge this is the first time that a detailed study on the electrospinning time dependent behaviour on the density of ZnO based fibers and subsequent in situ alignment of a single graphene ZnO nanofiber composite for UV sensing has been reported.

2 Experimental

2.1 Materials

Polyacrylonitrile (PAN, Mw 150 000), Dimethylformamide (DMF), Zinc acetate dihydrate (ZnAc) were purchased from Sigma Aldrich. Graphene flakes were procured from Graphene-supermarket, USA. Positive photoresist S1813 and its corresponding developer was procured from Shipley Inc. USA. All chemicals were analytical pure and were used as received without any further purification. DI water Millipore system (~ 18.2 MΩ) was used throughout the experiment.

2.2 Sensor design and fabrication

Microfabricated gold electrodes were fabricated on highly doped p type silicon wafer using the cleanroom facilities available at IIT Hyderabad, India. Briefly, a 300 nm SiO_2 was grown on a (100) oriented p-type substrate by thermal oxidation technique to insulate the substrate. It was followed by spin coating positive photoresist S1813 to define the source and drain areas by photolithography. Chromium layer (20 nm) for adhesion and gold layer (180 nm) were deposited by DC sputtering. Finally, the electrodes were patterned by lift-off technique by ultra-sonicating with acetone. The radius and gap of the electrodes were fixed at 100 µm and 50 µm, respectively.

2.3 Preparation of electrospun Gr-ZnO nanofiber

Gr-ZnO nanofiber were synthesized according to the following procedure. PAN (8 wt. %) and ZnAc (10 wt. %) were dissolved in DMF. The mixture was stirred for 2 hours at room temperature. Thereafter different weight percentages of graphene flakes i.e. 0.2 wt. %, 0.5 wt. % and 0.8 wt. % were added to the solution and stirred for 24 hours at room temperature to obtain a homogeneous viscous solution ready for electrospinning. The electrospinning set up consists of a syringe, needle, grounded collector and high voltage supply. ZnO and Gr-ZnO solutions were electrospun on fabricated gold electrodes patterned on Si-SiO_2 substrate at room temperature. The patterned electrodes were kept 10 cm away from tip of the needle of 24 gauge. Voltage applied between the needle and grounded collector was maintained at 18kV with a constant flow rate of 8µL/min. In addition to the standard electrospinning parameters, the operating time for electrospinning, was optimized to obtain a single aligned nanofiber between the pre patterned electrodes. Operating time for the current study was optimized to be in the range of 3-5 seconds which produced well aligned single

RSC Advances Accepted Manuscript

This journal is © The Royal Society of Chemistry 20xx

Please do not adjust margins

View Article Online
DOI: 10.1039/C5RA15351D

Published on 16 September 2015. Downloaded by UNIVERSITY OF NEBRASKA on 16/09/2015 15:31:34.

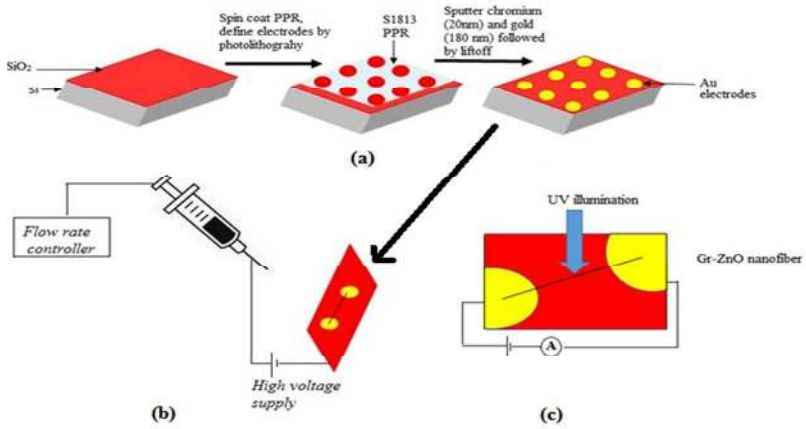

Fig 1: a) Schematic of the microfabrication of gold electrodes b) Electrospinning with collector as pre patterned electrode c) UV sensing with single aligned Gr-ZnO nanofiber device.

Gr-ZnO nanofiber between the gold electrodes. Thereafter the devices were calcined at various temperature such as 400°C, 500°C and 600°C to remove the organic contents and residues. The complete process which includes fabrication of gold electrode by photo¬lithography and electrospinning is pictorially shown in fig1.

2.4 Device characterization and sensing

Field emission scanning electron microscopy, ZEISS Ultra-55 Scanning Electron Microscope, was used to study the surface morphology of the Gr-ZnO nanofibers and to determine the diameter range of the fibers at various calcination temperatures. The electric conductivity of a single nanofiber was measured by using cascade two-probe method, the current through the sample was measured with a Keithley 4200 SCS. The sample was measured four times in different directions by applying the potential of -1.0 to +1.0 V and average value of resistance was calculated. Raman studies were carried on a Senterra inVia opus Raman spectrometer (Senterra, Bruker, UK) using 532 nm excitation and the optical power delivered onto the sample was 10 mW/cm^2. XRD studies (X'pert PRO) were performed using Cu Kα radiation. The electrical measurements with UV illumination were performed by a custom assembled UV light of 12 W.

3 Results and discussions

Electrospinning of Gr-ZnO composite was carried out at different time intervals so as to observe the time dependence behaviour on the alignment of fibers between the electrodes. Operating time of electrospinning was varied from 15 seconds to 2 seconds. Fig 2 shows SEM images of the device wherein the nanofibers are electrospun for 15, 12, 8, 4 seconds. As the operating time for electrospinning was decreased from 15 seconds to 4 seconds, randomly arranged high density nanofibers were converted to perfectly aligned single nanofiber across the electrodes. For 15 seconds, a dense network of fibers randomly arranged between the electrodes was observed. With decrease of the electrospinning time to 12 seconds, there was a significant reduction in the number of the fibers between the electrodes which still maintained random orientation. Fibers electrospun for 7 seconds showed further improvement in the arrangement and alignment of the fibers. Finally, at 4 seconds we observed a single fiber aligned perfectly between the electrodes. The procedure was repeated several times (7 times) and 3-5 seconds period was found to be the optimum period for aligning a single fiber. A suitable explanation to this phenomenon of variation in the optimized time can be attributed to several physical parameters such as temperature, humidity etc.

RSC Advances Accepted Manuscript

Please do not adjust margins
View Article Online
DOI: 10.1039/C5RA15351D

Published on 16 September 2015. Downloaded by UNIVERSITY OF NEBRASKA on 16/09/2015 15:31:34.

which affects the solvent evaporation rate and viscosity thereby changing the working parameters of electrospinning. This result was in close agreement with the work done by *Sharma et al* [20] wherein they reported the alignment of the 1-5 carbon nanowires with the time to be in range of 3-5 seconds with the help of rotating drum. The use of rotating drum in alignment on the pre patterned electrodes is not suggested as the position of the pre patterned electrodes changes continuously thus making it difficult for getting aligned fiber between the pre patterned electrodes. Further, in that study, focused ion beam was used to discard extra carbon fibers if any. In the present study we optimized the parameters by carefully studying the density of fibers between the pre patterned electrodes electrospun at various operating times. For all the above mentioned operating times, optimized electrospinning parameters as mentioned in the experimental section were kept constant. Fig 3 shows the near linear relationship between the number of fibers between the electrodes and operating time for 0.5 wt. % of graphene. As the electrospinning time increases we observe gradual curling behaviour of the fibers which is in agreement to reports where the operating time of the electrospinning is kept high.

Composite nanofibers synthesized at 4 seconds electrospinning time were calcined at different temperatures to study the morphology of the fibers with increasing temperature. Fig 4a and fig 4b show the high magnification SEM image of pure ZnO and Gr-ZnO nanofiber both calcined at 400°C respectively.

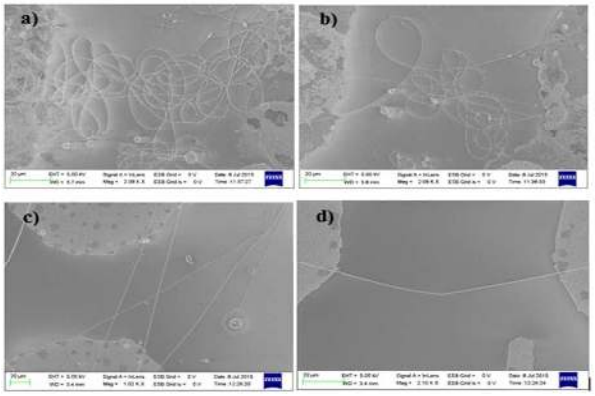

Fig 2: SEM images of the device electrospun for various time segments a) 15 seconds b) 12 seconds c) 7 seconds d) 4 seconds. As time deceases from 15 seconds, randomly arranged composite nanofibers were converted to perfectly single aligned composite nanofiber between the pre patterned gold electrode.

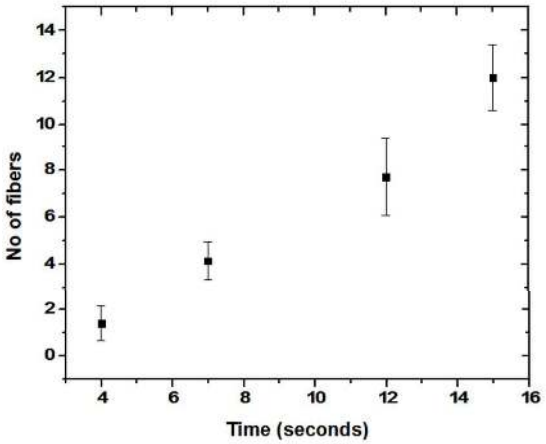

Fig 3: Graph demonstrating the near linear relation between no. of fibers and operating time of electrospinning for 0.5 wt. % of graphene.

Pure ZnO nanofiber exhibits smooth surface morphology, whereas composite shows flakes like structure uniformly all over the surface of ZnO nanofiber. The morphology of the composite as seen from fig 4b is ZnO nanofiber embedded in graphene flakes. Furthermore, as can be clearly seen, the flakes are transparent, which is an inherent property of graphene. Diameter and morphology of the composite fibers changes based on the composition of the solution used for electrospinning. Upon addition of graphene, conductivity of the solution changes. Since the synthesis of the composite is by electrospinning, conductivity of the solution is an important parameter in determining the nanofiber diameter. In electrospinning, stretching of the polymer solution is caused by repulsion of charges at its surface. Hence when the conductivity increases, more charges are carried by electrospinning jet which causes the polymer solution to stretch more, thereby decreasing the diameter. In our work, upon addition of graphene, the conductivity of the solution increases and this in turn decreases the overall diameter and morphology of the composite. This observation is in agreement with various studies reported on electrospinning[21, 22]. In addition, the initial dispersion of graphene is an important parameter that affects the nanofiber diameter and morphology[23-26]. It is evident from fig 4a and fig 4b that initial graphene concentration in the electrospinning solution affects both diameter as well as morphology of the nanofiber. As can be seen from fig 4b, graphene is uniformly dispersed all over the surface of ZnO proving that 0.5 wt. % of graphene is sufficient to form a

RSC Advances Accepted Manuscript

This journal is © The Royal Society of Chemistry 20xx
Please do not adjust margins

View Article Online
DOI: 10.1039/C5RA15351D

Published on 16 September 2015. Downloaded by UNIVERSITY OF NEBRASKA on 16/09/2015 15:31:34.

uniform dispersion. The dispersion of higher wt. % of graphene was not studied as a UV sensor demands dark current to be low. Increasing the graphene content increases the dark current thereby affecting the sensitivity of the sensor. This has been explained in the later part of the discussions where optimization studies to select the optimum Gr/ZnO composition for UV sensing have been discussed.

To study the effect of calcination temperature on the composite, fibers were calcined at elevated temperatures of 500°C and 600°C. Fig 4c and fig 4d show the Gr-ZnO composite high magnification image calcined at 500°C and 600°C respectively. As can be clearly seen, there is a decrease in the fiber diameter (~ 250 nm) and also the flake size. The decrease in the nanofiber diameter can be attributed to the decomposition and evaporation of organic components and residues. The decrease in the flake size of graphene is caused due to burning of carbon content at high temperatures which is evident from the raman spectra of the composite nanofiber calcined at 600°C (Fig S1 in supplementary information) which further decreases the overall diameter of the nanofiber[27]. Hence the optimized composite nanofiber calcined at 400°C was chosen for UV sensing application because of the higher graphene content.

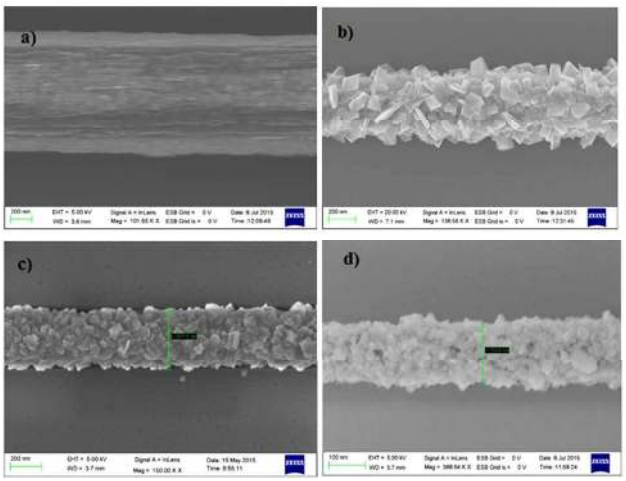

Fig 4: High magnification SEM images showing the morphology of the fibres calcined at various temperatures a) Pure ZnO calcined at 400°C b) Gr-ZnO calcined at 400°C c) Gr-ZnO calcined at 500°C d) Gr-ZnO calcined at 600°C. As calcination temperature increases, decrease in the nanofiber diameter and flake size was observed.

Fig 5 shows high magnification SEM images at the contact of gold electrodes and Gr-ZnO composite nanofiber. The image was taken at 45° tilt to ascertain that uniform contact has been established between the fiber and the metal electrode which minimizes the contact resistance between the two thereby enhancing transfer of electrons from composite nanofiber to gold contact and vice-versa. This was achieved by calcination after the in-situ alignment of fiber which stabilizes the contact. I-V curves recorded further confirmed the near ohmic contact. The in-situ alignment of fibers is advantageous in forming near ohmic contact which involves heating of both electrode as well as nanofiber simultaneously thus discarding the additional heating steps often required when the electrodes are fabricated after the electrospinning process.

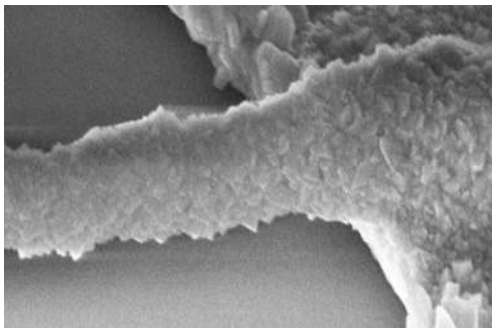

Fig 5: SEM image of contact between the Gr-ZnO and gold electrode

Fig 6 reveals the X-ray diffraction (XRD) pattern of the graphene, pure ZnO nanofibers and Gr-ZnO nanofiber composite calcined at 400°C in the range $20^{o} < 2\theta < 60°$. 2θ peaks at 31.8 (100), 34.4 (002), 36.3 (101), 47.5 (102) and 56.6 (110) indicate the hexagonal wurtzite crystal structure of ZnO nanofibers. The diffraction peaks at 26.1 and 54.71 denoted by G (002) and G (004) respectively, indicate the crystal planes of graphene. The broad graphene peak at 26.1 in the Gr-ZnO XRD spectra indicates amorphous carbon, which is due to defects induced by addition of ZnO. Also, the intensity of peak being weak can be attributed to low concentration of graphene in the composite. The XRD data thus confirms high crystallinity of Gr-ZnO composite nanofibers.

RSC Advances Accepted Manuscript

Please do not adjust margins
View Article Online
DOI: 10.1039/C5RA15351D

Published on 16 September 2015. Downloaded by UNIVERSITY OF NEBRASKA on 16/09/2015 15:31:34.

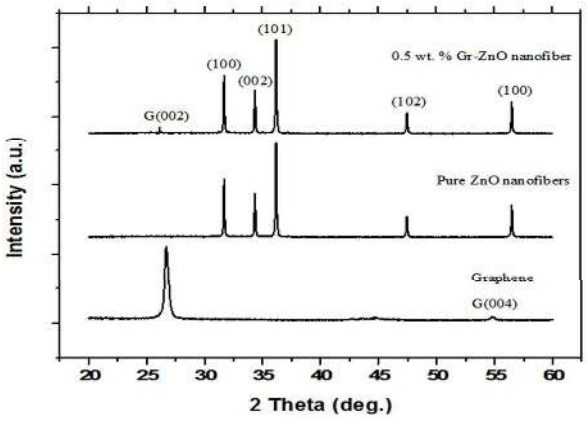

Fig 6: XRD spectrum of graphene, pure ZnO nanofibers and 0.5 wt. % of Gr-ZnO nanofiber composite calcined at 400°C.

Detailed chemical/molecular analysis was performed in terms of Raman spectroscopy to confirm the composite formation. Fig 7 represents the Raman spectra of the Gr-ZnO composite with 0.5 wt. % of graphene flakes. The well know G peak (~1574 cm^{-1}) which is characteristic for sp^2 hybridized carbon peak is well evident. The other peak which is at ~ 1359 cm^{-1} denoted as D band which originates from structural imperfections is also prominent. The intensity of D peak greater than G peak also confirms the formation of composite due to increased disorder caused due to addition of ZnO. Also, the addition of ZnO in the graphene makes it amorphous which causes the G peak peak intensity to be low and not uniform[13]. .With 0.5 wt. % of graphene in the composite, typical Raman peaks of ZnO disappear. This is due to large number of graphene flakes embedded in the ZnO nanofiber which conceals the Raman signals of ZnO.

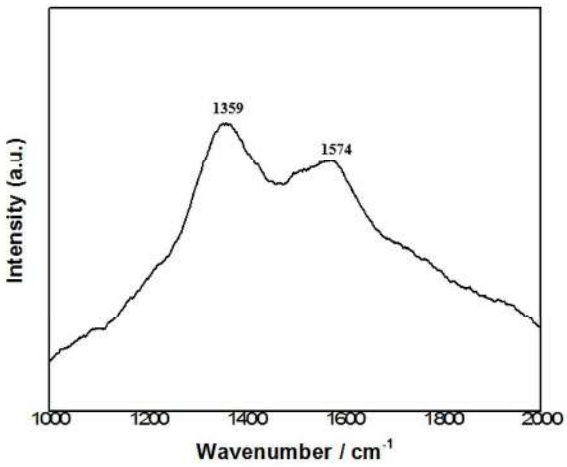

Fig 7: Raman spectra of Gr-ZnO composite with 0.5 wt. % of Gr calcined at 400°C.

As a part of optimization studies to select the optimum Gr/ZnO composition, 3 different weight percentages of graphene flakes i.e. 0.2 wt. %, 0.5 wt. % and 0.8 wt. % were used to synthesize the composites and subsequent UV sensing was performed. It was found that for the sample containing 0.2 wt. % of graphene, the dark current value recorded was the least but upon UV exposure the resulting current saturated after 30 minutes thus yielding ~ 586 fold change in conductance as opposed to ~ 1892 fold change for sample with 0.5 wt. % of graphene. For 0.8 wt. % graphene, the dark current recorded was high making it unsuitable for UV sensing applications. Hence, in order to achieve better sensitivity, 0.5 wt. % graphene composition was selected to synthesize the composite. The figures demonstrating the dark resistance values measured as a function of different compositions and I-V response of a typical device with 0.2 wt. % of graphene can be found in the supplementary information (Figures S2 and S3 respectively). Fig. 8 shows the current – voltage (I-V) response of a typical single aligned Gr-ZnO composite nanofiber device at 0.5 wt. % of Gr calcined at 400°C. The reason for choosing sample calcined at 400°C was greater flake size visibility in the SEM images, explaining more graphene presence which helps in enhancing the transport properties of the photogenerated electrons. Moreover graphene decomposes above 500°C, which is evident from the raman spectra as discussed earlier in this section. I-V response under UV illumination was taken at 5, 15, 30, 45 minutes to study the response of current with time. Under UV illumination, electron-hole pair are generated when the energy of illumination is greater than

RSC Advances Accepted Manuscript

This journal is © The Royal Society of Chemistry 20xx
Please do not adjust margins

View Article Online
DOI: 10.1039/C5RA15351D

Published on 16 September 2015. Downloaded by UNIVERSITY OF NEBRASKA on 16/09/2015 15:31:34.

or equal to band gap of ZnO. For pure ZnO, photogenerated electrons tends to recombine which decreases the carrier lifetime and hence the current. Hence the need for graphene as a transport material arises for capturing the photogenerated electrons, thereby preventing them from recombination, ultimately increasing the carrier lifetime. In case of Gr-ZnO nanofiber composite, since work function of graphene is less than conduction band of ZnO[28], photogenerated electrons get readily transferred to graphene, and higher electron mobility of graphene enables faster collection of charge carriers at the gold electrodes, thereby enhancing the carrier lifetime of the photogenerated electrons. For pure ZnO nanofibers, in the absence of UV light there is formation of depletion layer due to oxidation of n type ZnO nanofibers by adsorption of atmospheric oxygen molecules thereby decreasing the conductivity[29]. Before starting to measure the current under UV illumination, samples were kept in dark for 12 hours so as to stabilize. Under exposure to UV light for 5 minutes there is 69% decrease in the resistance for 0.5 wt. % of graphene respectively indicating a quick response to the UV illumination for both devices. After 15 minutes, 98.67 % decrease in resistance for 0.5 wt. % of graphene was observed. This increase in conductance can be attributed to faster collection of photogenerated electrons by graphene. As the time of illumination was increased to 30 minutes, 99.8% and finally at 45 minutes, 99.9 % decrease in the resistance was observed. As time increases, the amount of photogenerated electrons transferring to graphene increases thereby increasing the current. After 30 minutes of UV exposure, the decrease in the resistance is less compared to the decrease in 15-30 minutes for 0.5 wt. % of graphene and it saturates after 40 to 45 minutes of UV illumination. The above phenomena can be attributed to the decomposition of graphene due to photogenerated hole and electrons, which react with the atmospheric oxygen and moisture, thereby forming oxygen reactive species which oxidizes graphene[30].

Fig. 9 provides a schematic representation of the process. Photogenerated electrons tends to transport towards the gold electrode due to very high charge transport mobility of graphene, but few electrons react with atmospheric oxygen and forms O_2 radicals. Also, the photogenerated holes react with the atmospheric oxygen and form hydroxyl (OH) radical. These oxygen reactive species generated at the surface of the graphene are responsible for oxidation of graphene, thereby reducing the carbon content and increasing the oxygen content, hence saturating the conductivity. There have been few studies reporting the use of ZnO graphene composite for UV sensing. *Dang et al*[31] fabricated phototransistor with channel based on vertical ZnO nanorods and graphene. *Boruah et al*[32] demonstrated UV sensor based on ZnO nanowire grown on graphene foam. *Fu et al*[33] reported high performance single ZnO nanowire using chemical vapor deposition sandwiched between graphene sheets with on-off ratio of 800.

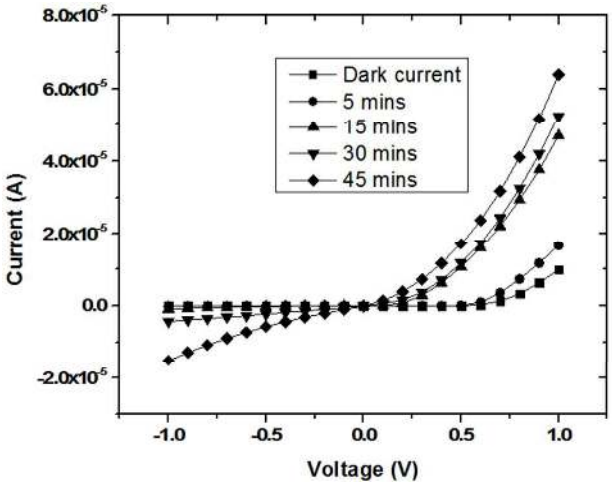

Fig 8: I-V curves of a typical Gr-ZnO device at 0.5 wt. % of Gr with and without UV illumination at various time instants.

RSC Advances Accepted Manuscript

Please do not adjust margins
View Article Online
DOI: 10.1039/C5RA15351D

Journal Name

ARTICLE

Published on 16 September 2015. Downloaded by UNIVERSITY OF NEBRASKA on 16/09/2015 15:31:34.

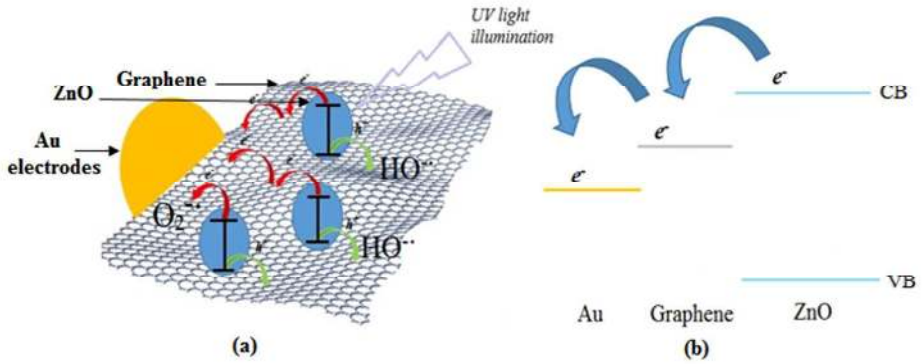

Fig 9: a) Schematic of the charge separation of photogenerated electrons and holes and their role in oxidation of graphene under UV illumination b) Band structure of Gr-ZnO nanofiber composite with gold electrodes

Liang et al[34] demonstrated one step synthesis of SnO_2/Graphene nanocomposite by solvothermal method for application in Li-Ion batteries, but in our approach we demonstrated in a single step, not only the in situ synthesis of ZnO/graphene nanofiber but also the alignment of a single composite fiber across the electrodes thus integrating into a device. This controlled approach in synthesis and precise positioning of the fiber can be performed simultaneously across multiple electrodes on a wafer thus making this technique suitable for large scale commercial applications.

Zhang et al[35] synthesized ZnO nanowire using electrodeposition method with transparent graphene contact. *Chang et al*[36] demonstrated the use of ZnO nanorod/graphene composite by solution growth method which was then drop casted between metal electrodes. *Wang et al*[37] fabricated flexible UV sensor with reduced graphene oxide ZnO composite synthesized by hydrothermal method. Unlike most of the above mentioned works, which involve working with high density nanofibers in forms of mats, nanorods, complex fabrication techniques such as defining electrodes using E-beam lithography, transfer process or drop casting which in ideal conditions too will lead to device to device variation, our work involves a simple, reproducible approach for one step in situ alignment of graphene-ZnO using electrospinning. The method is advantageous as it allows for precise manipulation of the resistance of sensor upon UV exposure by aligning single composite nanofiber across electrode. In addition, the current work employs two terminal device configuration which can be easily integrated further for an all-electronic readout signal for real time applications.

4 Conclusions

In summary, a facile, one step in situ single aligned graphene-ZnO nanofiber composite based UV sensor was developed. Time dependent behaviour on the alignment of nanofibers was studied and was optimized for alignment of single fiber across the pre patterned electrodes. Structural and chemical characterization revealed that uniform morphology of the composite consists of ZnO

RSC Advances Accepted Manuscript

Please do not adjust margins

View Article Online
DOI: 10.1039/C5RA15351D

Published on 16 September 2015. Downloaded by UNIVERSITY OF NEBRASKA on 16/09/2015 15:31:34.

embedded in graphene flakes throughout the surface of the fiber. It was observed that approximately 4 seconds of electrospinning time is required for obtaining a perfectly aligned single graphene-ZnO fiber. Under UV illumination for 45 minutes, significant decrease in the resistance of the device was observed. Our proposed approach for in situ aligned composite provides a simple, cost effective alternative for developing an integrated UV sensor and can be extended for a variety of other sensing applications.

Acknowledgements

A part of the reported work (characterization) was carried out at the IITBNF, IITB under INUP which is sponsored by DeitY, MCIT, Government of India.

References

1. Razeghi, M., & Rogalski, A, *Journal of Applied Physics*, **1996**, 79(10), 7433-7473.
2. Huang, M. H., Mao, S., Feick, H., Yan, H., Wu, Y., Kind, H & Yang, P, *Science*, **2001** 292(5523), 1897-1899.
3. Basu, S., & Dutta, A, *Sensors and Actuators B: Chemical*, **1994**, 22(2), 83-87.
4. Wan, Q., Li, Q. H., Chen, Y. J., Wang, T. H., He, X. L., Li, J. P., & Lin, C. L, *Applied Physics Letters*, **2004**, 84(18), 3654-3656.
5. Sernelius, B. E., Berggren, K. F., Jin, Z. C., Hamberg, I., & Granqvist, C. G , *Physical Review B*, **1988**, 37(17), 10244.
6. Yousef, A., Barakat, N. A., Amna, T., Unnithan, A. R., Al-Deyab, S. S., & Kim, H. Y., *Journal of Luminescence*, **2012**, 132(7), 1668-1677.
7. Bai, S., Wu, W., Qin, Y., Cui, N., Bayerl, D. J., & Wang, X., *Advanced Functional Materials*, **2011**, 21(23), 4464-4469.
8. Hoa, L.T., Tien,H.N., Hur, S.H., *Sensors and Actuators A: Physical*, **2014**, 207, 20-24.
9. Li, H. G., Wu, G., Chen, H. Z., & Wang, M., *Sensors and Actuators B: Chemical,* **2011**, 160(1), 1136-1140.
10. Xi, M., Wang, X., Zhao, Y., Zhu, Z., & Fong, H., *Applied Physics Letters,* **2014**, 104(13), 133102.
11. Akhavan, O., *ACS nano*, **2010**, 4(7), 4174-4180.
12. Hwang, J. O., Lee, D. H., Kim, J. Y., Han, T. H., Kim, B. H., Park, M., Kim, S. O., *Journal of Materials Chemistry*, **2011**, 21(10), 3432-3437.
13. An, S., Joshi, B. N., Lee, M. W., Kim, N. Y., & Yoon, S. S., *Applied Surface Science*, **2014**, 294, 24-28.
14. Dong, X., Cao, Y., Wang, J., Chan-Park, M. B., Wang, L., Huang, W., & Chen, P., *RSC Advances*, **2012**, 2(10), 4364-4369.
15. Zhou, X., Shi, T., & Zhou, H., *Applied surface science*, **2012**, 258(17), 6204-6211.
16. Yin, Z., Wu, S., Zhou, X., Huang, X., Zhang, Q., Boey, F., & Zhang, H., *Small*, **2010**, 6(2), 307-312.
17. Xu, S., & Wang, Z. L., *Nano Research*, **2011**, 4(11), 1013-1098.
18. Stafiniak, A., Boratyński, B., Baranowska-Korczyc, A., Fronc, K., Elbaum, D., & Tłaczała, M., *Journal of the American Ceramic Society,* **2014**, 97(4), 1157-1163.
19. Allen, M. J., Tung, V. C., & Kaner, R. B., *Chemical reviews,* **2009**, 110(1), 132-145.
20. Sharma, S., Sharma, A., Cho, Y. K., & Madou, M., *ACS applied materials & interfaces,* **2012**, 4(1), 34-39.
21. Angammana, C. J., & Jayaram, S. H., *IEEE Transactions on Industry Applications*, **2011**, 47(3), 1109-1117.
22. Tan, S. H., Inai, R., Kotaki, M., & Ramakrishna, S. *Polymer*, **2005**, 46(16), 6128-6134.
23. Davis, V. A., Parra-Vasquez, A. N. G., Green, M. J., Rai, P. K., Behabtu, N., Prieto, V.,& Pasquali, M, *Nature nanotechnology*, **2009**, 4(12), 830-834.
24. Xu, T., & Davis, V. A, *Langmuir*, **2014**, 30(16), 4806-4813.
25. Jiang, C., Saha, A., Young, C. C., Hashim, D. P., Ramirez, C. E., Ajayan, P. M., & Martí, A. A, *ACS nano*, **2014**, 8(9), 9107-9112.
26. Jiang, C., Saha, A., Xiang, C., Young, C. C., Tour, J. M., Pasquali, M., & Martí, A. A, *ACS nano*, **2014**, 7(5), 4503-4510.
27. Pramoda, K., Suresh, S., Matte, H. R., & Govindaraj, A., *Bulletin of Materials Science*, **2013**, 36(4), 585-590.
28. Roy, P., Periasamy, A. P., Liang, C. T., & Chang, H. T., *Environmental science & technology,* **2013**, 47(12), 6688-6695.
29. Kind, H., Yan, H., Messer, B., Law, M., & Yang, P., *Advanced materials,* **2002**, 14(2), 2002, 158.

RSC Advances Accepted Manuscript

Please do not adjust margins
View Article Online
DOI: 10.1039/C5RA15351D

30. Mun, D. H., Lee, H. J., Bae, S., Kim, T. W., & Lee, S. H., *Physical Chemistry Chemical Physics*, **2015**, 24(17), 15683-15686.
31. Dang, V. Q., Trung, T. Q., Duy, L. T., Kim, B. Y., Siddiqui, S., Lee, W., & Lee, N. E., *ACS applied materials & interfaces,* **2015**, 7(20), 11032–11040.
32. Boruah, B. D., Mukherjee, A., Sridhar, S., & Misra, A., *ACS applied materials & interfaces,* **2015**, 7(19), 10606–10611.
33. Fu, X. W., Liao, Z. M., Zhou, Y. B., Wu, H. C., Bie, Y. Q., Xu, J., & Yu, D. P., *Applied Physics Letters*, **2012**, 100(22), 223114.
34. Liang, J., Wei, W., Zhong, D., Yang, Q., Li, L., & Guo, L., *ACS applied materials & interfaces*, **2012**, 4(1), 454-459.
35. Zhang, H., Babichev, A. V., Jacopin, G., Lavenus, P., Julien, F. H., Egorov, A. Y., & Tchernycheva, M., *Journal of Applied Physics,* **2013**, 114(23), 234505.
36. Chang, H., Sun, Z., Ho, K. Y. F., Tao, X., Yan, F., Kwok, W. M., & Zheng, Z., *Nanoscale*, **2011**, 3(1), 258-264.
37. Wang, Z., Zhan, X., Wang, Y., Muhammad, S., Huang, Y., & He, J., *Nanoscale*, **2012**, 4(8), 2678-2684.

Published on 16 September 2015. Downloaded by UNIVERSITY OF NEBRASKA on 16/09/2015 15:31:34.

RSC Advances Accepted Manuscript

This journal is © The Royal Society of Chemistry 20xx

Please do not adjust margins